CHIN. PHYS. LETT. Vol. 27, No. 8 (2010) 085201

A Comparison Study of Three CESE Schemes in MHD Simulation *

JI Zhen(纪珍)[1,2**], ZHOU Yu-Fen(周玉芬)[1]

[1]*State Key Laboratory of Space Weather, Center for Space Science and Applied Research, Chinese Academy of Sciences, Beijing 100190*

[2]*Graduate School, Chinese Academy of Sciences, Beijing 100049*

(Received 28 January 2010)

The space-time conservation element and solution element (CESE) scheme is a new second order numerical scheme based on the concept of space-time conservation integration. In order to further overcome excessive numerical damping due to small Courant–Friedrichs–Lewy (CFL) number and to obtain a high quality solution, a Courant number insensitive (CNIS) scheme and a high-order scheme have been proposed by Chang et al. for fluid mechanics problems recently. In this study, to explore the potential capability of applications of the CNIS CESE scheme and the high-order CESE scheme to magnetohydrodynamics (MHD) equations, several benchmark MHD problems are calculated in one and two dimensions: (i) Brio and Wu's shock tube, (ii) Dai and Woodward's case, (iii) the Orszag–Tang vortex problem, (iv) the Riemann problem. The numerical results just prove that the CNIS scheme is more accurate and can keep the divergence free condition of the magnetic field, even if the CFL number is $\ll 1$. Meanwhile, the tests show that the high order CESE scheme possesses the ability to solve MHD problems but is sensitive to the Courant number.

PACS: 52.30.Cv, 95.30.Qd DOI: 10.1088/0256-307X/27/8/085201

The conservation element and solution element (CESE) method was originally reported by Chang and his co-workers in the 1990s.[1−3] It differs thoroughly from the traditional well-established methods in both principle and methodology, including: (i) treating space and time as an entity, (ii) excluding the characteristics-based techniques (such as Riemann solvers), (iii) solving the physical variables and their spacial derivatives simultaneously, (iv) making the introduced damping effect controllable. It has been widely used in fluid mechanics and magnetohydrodynamics (MHD) problems, such as detonations, magnetic reconnection, etc.[3−8] In all these former studies, the numerical results agree well with those obtained by using other traditional schemes and indicate that the CESE method not only has high resolution but also can capture both sharp shock and small disturbances.

The CESE method becomes more dissipative while the Courant number is much less than one. Thus, Chang *et al.*[9] constructed the Courant number insensitive (CNIS) CESE method by reforming the calculation technique of spacial derivative of the physical variables to overcome this disadvantage. The CNIS CESE scheme has been used in hydromechanics and the numerical results indicated that the new scheme is accurate and stable with a large range of the Courant number, even if the Courant number is $\ll 1$.[10] In this study, the Courant number is changed between 0.00088 and 0.88.

On the other hand, in order to obtain accuracy more than second order, Chang *et al.*[11,12] proposed the high order scheme referred as $\alpha(3)$ and $\alpha(4)$ scheme. Some researchers adopted the principle of the $\alpha(3)$ scheme by changing the method of calculating the derivative.[13,14] The high order CESE scheme has been used to simulate fluid problems and the results was more precise.[11−13] In this Letter, the applicability of the high order scheme from the standpoints of accuracy and efficiency is discussed by some benchmark problems. In the following paragraphs we will briefly describe the three kinds of CESE methods mentioned above.

Consider the one-dimension ideal MHD equations

$$\frac{\partial \boldsymbol{U}}{\partial t} + \frac{\partial \boldsymbol{F}}{\partial x} = 0, \tag{1}$$

where

$$\boldsymbol{U} = \begin{pmatrix} \rho \\ \rho u \\ \rho v \\ \rho w \\ e \\ B_y \\ B_z \end{pmatrix}, \quad \boldsymbol{F}(U) = \begin{pmatrix} \rho u \\ \rho u^2 + p_0 - B_x^2 \\ \rho uv - B_x B_y \\ \rho uw - B_x B_z \\ F_5 \\ uB_y - vB_x \\ uB_z - wB_x \end{pmatrix},$$

$$F_5 = (e + p_0)u - B_x(uB_x + vB_y + wB_z), \tag{2}$$

where ρ is the density, (u, v, w) is the flow speed, (B_x, B_y, B_z) is the magnetic field, total energy $e = p/(\gamma - 1) + \rho(u^2 + v^2 + w^2)/2 + (B_x^2 + B_y^2 + B_z^2)/2$ and the total pressure $p_0 = p + (B_x^2 + B_y^2 + B_z^2)/2$.

*Supported by the National Natural Science Foundation of China under Grant Nos 40904050 and 40874077, and the Specialized Research Fund for State Key Laboratories.

**Email: zji@spaceweather.ac.cn

According to some papers,[1−3] x and t are considered as the coordinates of a two-dimensional Euclidean space E_2. By using Gauss' divergence theorem in the spacetime E_2, Equation (1) can be written as the integral conservation form

$$\oint_{s(v)} h \cdot d\boldsymbol{s} = 0, \tag{3}$$

where $h = h(\boldsymbol{u}, F(\boldsymbol{u}))$ represents the flux vectors, $s(v)$ is the boundary of an arbitrary region v, $d\boldsymbol{s}$ is the product of the outward unit normal and the area of a surface element on $s(v)$.

As referred in Refs. [1,4,5,15], the total computation region is divided into non-overlapping conservation elements (CEs). Each solution element (SE) includes a vertical line segment, a horizontal line segment and their neighborhood which are the vicinity of the solution points. The surfaces of $\mathrm{SE}(j,n)$ and $\mathrm{SE}(j-\frac{1}{2}, n-\frac{1}{2})$ form the $\mathrm{CE}_-(j,n)$, while surfaces of $\mathrm{SE}(j,n)$ and $\mathrm{SE}(j+\frac{1}{2}, n-\frac{1}{2})$ form the $\mathrm{CE}_+(j,n)$ (refer to Fig. 1(a)).

For any $(x,t) \in \mathrm{SE}(j,n)$, the flow variables $u^*(x,t;j,n)$ and fluxes $F^*(x,t;j,n)$ are approximated by the first-order Taylor series expansion. Integrating Eq. (3) on the surfaces of CE_- and CE_+ and substituting u^* and F^* into it, one can obtain[1−3]

$$u_j^n = \frac{1}{2}\left(u_{j-1/2}^{n-1/2} + u_{j+1/2}^{n-1/2} + s_{j-1/2}^{n-1/2} - s_{j+1/2}^{n-1/2}\right), \tag{4}$$

where

$$s_j^n = \frac{\Delta x}{4}(u_x)_j^n + \frac{\Delta t}{\Delta x}\left[f_j^n + \frac{\Delta t}{4}(f_t)_j^n\right]. \tag{5}$$

According to Eq. (4), one can obtain u_j^n at new time level. The derivatives are calculated as follows:[4]

$$(u_x^{\pm})_j^n = \frac{u_{j\pm1/2}^n - u_j^n}{x_{j\pm1/2} - x_j}; \quad (u_x)_j^n = \boldsymbol{W}[(u_x^-)_j^n, (u_x^+)_j^n, \alpha];$$
$$\boldsymbol{W}\left[(x^-)_j^n, (x^+)_j^n, \alpha\right] = \frac{|x^+|^\alpha x^- + |x^-|^\alpha x^+}{|x^+|^\alpha + |x^-|^\alpha}, \tag{6}$$

where $\alpha = 0 \sim 2$. When $\alpha = 0$, the function becomes arithmetic mean. The introduction of parameter α leads to a source of numerical dissipation. The combination of Eqs. (4) and (6) is referred as the $a-\alpha$ scheme.

It is well known that the CESE method may be highly dissipative for a small Courant number. In order to overcome this disadvantage, the CNIS CESE method is introduced by Chang *et al.*[9] To be specific, some additional nodes are introduced into the basic grid. These nodes are expressed as P_-, M_-, M_+ and P_+, respectively (see Fig. 1(b)). $\mathrm{M}_\pm$ is the midpoint of the line segment (the centroids of quadrilaterals in two dimensions (2D)) between (j,n) and $(j \pm 1/2, n)$. The position of $\mathrm{P}_\pm$ is determined by local Courant number τ and the coordinates of the point $(j \pm 1/2, n)$. The point $\mathrm{P}_\pm$ will move from the point $(j \pm 1/2, n)$ to the point $\mathrm{M}_\pm$ while the value of local Courant number alters from 1 to 0. Assuming that $(x_\pm, t_n)$ represents the coordinates of the point $(j \pm 1/2, n)$, the relation is expressed as[10]

$$x_{P_\pm} = x_{M_\pm} + \tau(x_\pm - x_{M_\pm}). \tag{7}$$

As mentioned before, replacing $u_{j\pm1/2}$ with $u_{(p_\pm)}$ in Eq. (6), one will obtain $(u_x^\pm)_j^n$. The variables $u_{(p_\pm)}$ are defined as the first-order Taylor expansion series of $u_{j\pm1/2}^{n-1/2}$.

It is clear that the CNIS CESE method could be reduced into the $a-\alpha$ scheme while the Courant number is close to one, and into less dissipative a scheme when the Courant number approaches zero. As a result, the scheme is insensitive to the global Courant number which is the smallest local Courant number.

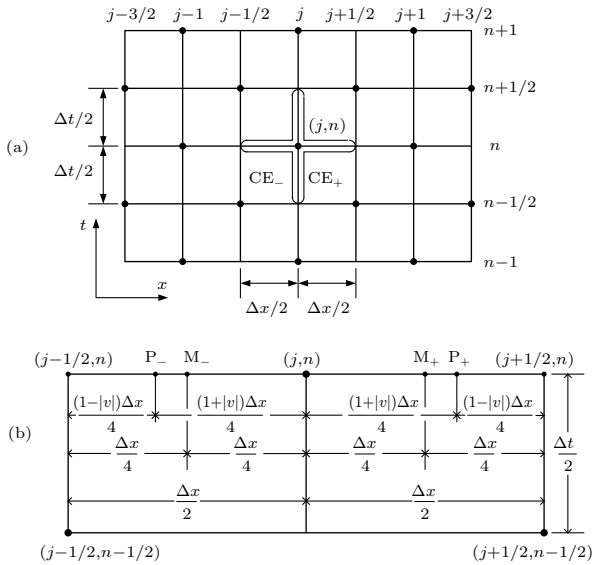

Fig. 1. (a) A basic grid of the CESE scheme, (b) definition of points P_-, M_-, M_+, P_+.

The original CESE method expands the physical variables with the first order Taylor series in SEs. In order to reach higher accuracy, Chang *et al.*[11,12] developed the high order scheme based on the high order Taylor series. Zhang *et al.*[14] changed the structure of CEs and SEs and obtained a simpler high-order CESE scheme. In this study, Zhang's method will be employed for our MHD benchmark problems. Zhang's second order CESE scheme can be stated as follows.

According to Eq. (1), one obtains $(u_t)_j^n = -(f_x)_j^n$, $(u_{xt})_j^n = -(f_{xx})_j^n$, $(u_{tt})_j^n = -(f_{xt})_j^n$. This implies that the independent variables are $u_j^n, (u_x)_j^n$ and $(u_{xx})_j^n$. Integrating Eq. (3) on the surfaces of two neighbored CEs and substituting the second-order Taylor expansion series into the integral equation, one will obtain the function for calculating u_j^n. The first partial derivative is defined as before. Using the dif-

ference method, $(u_{xx})_j^n$ can be defined by[14]

$$(u_{xx})_j^n = \boldsymbol{W}[(u'_{xx-})_j^n, (u'_{xx+})_j^n, \alpha];$$
$$(u'_{xx\pm})_j^n = \pm\frac{(u'_x)_{j\pm1/2}^n - (u_x)_j^n}{\Delta x/2} \quad (8)$$

additionally, $(u'_x)_{j\pm1/2}^n$ can be calculated by the first-order Taylor expansion series of $(u_x)_{j\pm1/2}^{n-1/2}$.

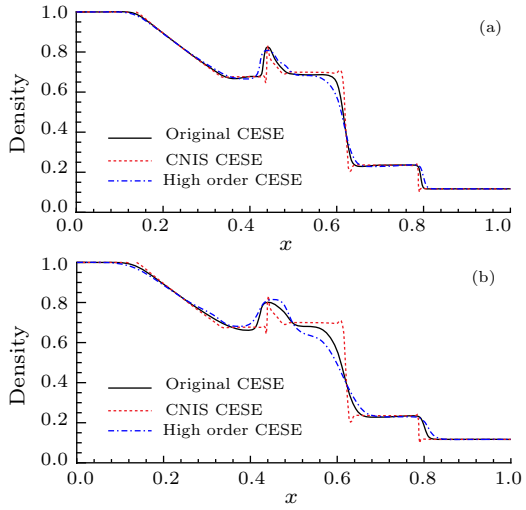

Fig. 2. Comparison of the density of the Brio–Wu shock tube problem at $t = 0.2$ for 800 grid points: (a) CFL = 0.0088, (b) CFL = 0.00088.

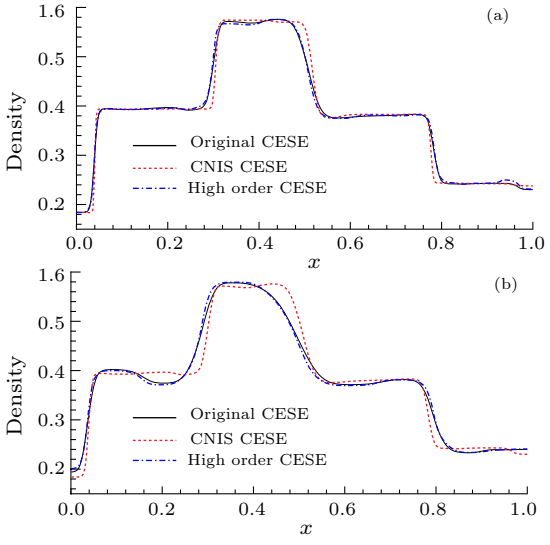

Fig. 3. Comparison of density of the Dai–Woodward problem at $t = 0.2$ for 800 grid points: (a) CFL = 0.0088, (b) CFL = 0.00088.

In this study, we calculate two shock tube problems in one dimension (1D),[15] vortex problem and Riemann problem in 2D respectively to investigate the capability of these methods. All the tests are solved with different Courant–Friedrichs–Lewy (CFL) numbers using these three CESE methods. When CFL= 0.88, 0.088, the results of these three schemes do not have obvious differences and are the same as those of other numerical schemes.[16] Figures 2 and 3 illuminate the comparison of the density of these two shock tube problems with CFL = 0.0088, 0.00088 at $t = 0.2$. In the figures, it is clearly seen that the CNIS CESE scheme can keep the accuracy of the results and reduce the numerical dissipation with very small CFL number. The overshoots in the figures can be reduced by using a larger value of α. However, the original CESE method and the high-order CESE scheme cannot accurately capture the shocks. To some extent, the result of the simplified second-order CESE scheme is sensitive to the CFL number.

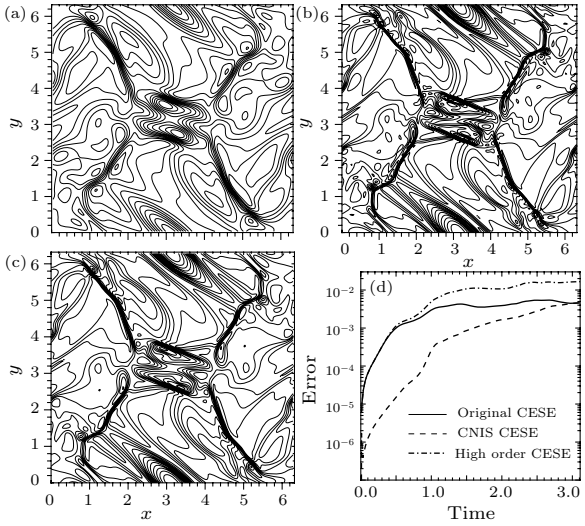

Fig. 4. Density of the Orszag–Tang vortex problem at $t = 3$ with CFL = 0.088 for 193×193 uniform grid points: (a) the original CESE scheme, (b) the CNIS CESE scheme, (c) the high-order CESE scheme, (d) the evolution of the error of the three schemes.

Figure 4 is the density of Orszag–Tang vortex[17] solved by these three kinds of CESE methods with CFL = 0.088 at $t = 3$. As shown in the figure, the original CESE scheme and the high-order CESE method are more dissipative than the CNIS CESE scheme when the CFL number is less than 0.1. Figure 4(b) clearly shows the shock structure captured by the CNIS CESE scheme. However, the original CESE method does not capture the shock effectively (Fig. 4(a)). The result of the high-order CESE method becomes dissipative with small CFL number and has some indistinct shock structure (Fig. 4(c)). Figure 5 is the pressure of the 2D Riemann problem with CFL = 0.088 at $t = 0.2$. The results show the same feature as the former ones. Figures 4(d) and 5(d) express the evolution of the error in three methods along with time, in which error = $\frac{\sum \nabla\cdot\boldsymbol{B}}{nx\times ny}$ (the denominator is the total number of simulation nodes). The CNIS CESE method keeps the error at the same order as the original CESE, and the error does not increase with time. The high-order CESE method cannot keep the divergence constraint condition effectively. The error

of the high-order CESE scheme is slightly larger than that of other two methods. The most likely reason for this property of high-order CESE method is that the difference method for calculating the derivatives is similar to that used in the original CESE method, but the shock discontinuities are more intense than that captured by the original CESE method. We consider that the present calculation methods used for spatial derivatives in high order CESE scheme may need further improvement.

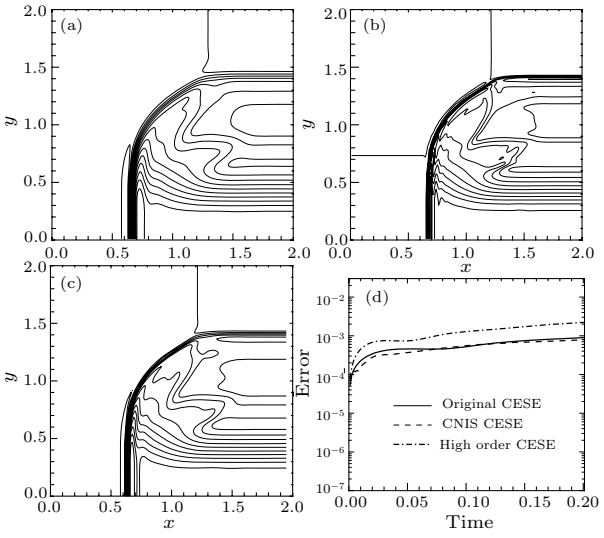

Fig. 5. Pressure of the Riemann problem at $t = 0.2$ with CFL $= 0.088$ for 193×193 uniform grid points: (a) the original CESE scheme, (b) the CNIS CESE scheme, (c) the high-order CESE scheme, (d) the evolution of the error of the three schemes.

In summary, the CNIS CESE method is the best of these three types of CESE schemes. When the CFL number is close to one, the CESE scheme and its two extensions can keep the accuracy of results and capture the shocks. However, when the CFL number is more or less than one, the original CESE scheme and the high-order scheme become dissipative and cannot solve the shocks accurately while the CNIS CESE scheme can keep the accuracy and the divergence constraint of the magnetic field. According to these conclusions, further applications of the CNIS CESE method to compute the MHD flow problems will be an emphasis in future work, such as its applications to magnetic reconnection, solar wind, propagation of waves, response of the Earth's atmosphere to solar wind, etc.[8,18,19]

References

[1] Chang S C 1995 *J. Comput. Phys.* **119** 295
[2] Chang S C, Wang X Y and Chow C Y 1998 *NASA* TM-1998-208843
[3] Chang S C, Wang X Y and Chow C Y 1999 *J. Comput. Phys.* **156** 89
[4] Zhang Z C and Yu S T 1999 *AIAA* Paper 1999-0904
[5] Zhang Z C, Yu S T and Chang S C 2002 *J. Comput. Phys.* **175** 168
[6] Feng X S, Hu Y Q and Wei F S 2006 *Sol. Phys.* **239** 235
[7] Feng X S, Zhou Y F and Wu S T 2007 *Astrophys. J.* **655** 1110
[8] Zhou Y F, Feng X S and Wu S T 2008 *Chin. Phys. Lett.* **25** 790
[9] Chang S C 2002 *AIAA* Paper 2002-3890
[10] Yen Joseph C and Wagner Donald A 2005 *AIAA* Paper 2005-2820
[11] Chang S C 2007 *AIAA* Paper 2007-5820
[12] Chang S C 2008 *NASA* TM-2008-215138
[13] Liu K X and Wang J T 2004 *Chin. Phys. Lett.* **21** 2085
[14] Zhang D L, Wang J T and Wang G 2009 *Chin. J. Comput. Phys.* **26** 211
[15] Zhang M J, Henry Lin S C and John Yu S T 2002 *AIAA* Paper 2002–3888
[16] Jiang G S, Wu C C 1999 *J. Comput. Phys.* **150** 561
[17] Zhang M J, John Yu S T and Henry Lin S C el at 2006 *J. Comput. Phys.* **214** 599
[18] Xiong M, Peng Z, Hu Y Q, Zheng H N 2009 *Chin. Phys. Lett.* **26** 015202
[19] Zheng H N, Zhang Y Y and Wang S et al 2006 *Chin. Phys. Lett.* **23** 399